Applied Surface Science 317 (2014) 19–25

Contents lists available at ScienceDirect

Applied Surface Science

journal homepage: www.elsevier.com/locate/apsusc

Nanostructured ZnO thin films prepared by sol–gel spin-coating

E. Heredia [a,*], C. Bojorge [a], J. Casanova [a], H. Cánepa [a], A. Craievich [b], G. Kellermann [c]

[a] UNIDEF (CONICET-MINDEF), J.B. de La Salle 4397, 1603 Villa Martelli, Pcia. de Buenos Aires, Argentina
[b] Instituto de Física, Universidade de São Paulo, Cidade Universitária, 66318 São Paulo, SP, Brazil
[c] Universidade Federal do Paraná, 19044 Paraná, Brazil

ARTICLE INFO

Article history:
Received 7 May 2014
Received in revised form 10 July 2014
Accepted 9 August 2014
Available online 19 August 2014

Keywords:
ZnO
Nanostructured thin films
XR
AFM
FESEM
GISAXS

ABSTRACT

ZnO thin films deposited on silica flat plates were prepared by spin-coating and studied by applying several techniques for structural characterization. The films were prepared by depositing different numbers of layers, each deposition being followed by a thermal treatment at 200 °C to dry and consolidate the successive layers. After depositing all layers, a final thermal treatment at 450 °C during 3 h was also applied in order to eliminate organic components and to promote the crystallization of the thin films. The total thickness of the multilayered films – ranging from 40 nm up to 150 nm – was determined by AFM and FESEM. The analysis by GIXD showed that the thin films are composed of ZnO crystallites with an average diameter of 25 nm circa. XR results demonstrated that the thin films also exhibit a large volume fraction of nanoporosity, typically 30–40 vol.% in thin films having thicknesses larger than ~70 nm. GISAXS measurements showed that the experimental scattering intensity is well described by a structural model composed of nanopores with shape of oblate spheroids, height/diameter aspect ratio within the 0.8–0.9 range and average diameter along the sample surface plane in the 5–7 nm range.

1. Introduction

Nanocrystalline ZnO is a material of great practical relevance because of its potential applications to the development of new gas and humidity sensors [1–3], UV detectors, optoelectronic devices [3,4], nanogenerators [5], etc. In addition, the porosity developed in ZnO thin films obtained by sol–gel favors other useful applications as substrates for catalysis, electrodes for solar cells, and for sensing of guest structures and biocompatible organic components.

The application to the development of conductive gas sensors composed of thin films of n-type zinc oxide is based on the dependence of the electrical characteristics of this material on the nature of the surrounding gas atmosphere. The performance of ZnO thin films as gas sensor depends on the internal microstructure of the material and on its surface geometry [6]. Thus, when this material is used as a gas sensor, a synthesis process leading to a controlled porous microstructure should be selected. Since the sensing process involves chemisorption, i.e. exchange of charges between adsorbed gaseous species and the metal oxide surface – the detailed characterization of the nanoporous structure of the materials is needed for adequate design of new sensor devices [6].

In a previous work, ZnO nanostructured films were obtained by the sol–gel technique [7], in this case drying the sample at room temperature after each deposit. The films prepared by this method are very porous, thin and flat, but their thicknesses are difficult to control.

In the present work, pure ZnO thin films were prepared by the sol–gel method and deposited by spin-coating. In this procedure the samples were submitted to successive heat treatments at 200 °C during 10 min after each deposit. This led to the consolidation of the different layers and to the proper control of the final film thickness.

The ZnO films were characterized by grazing-incidence X-ray diffraction (GIXD), atomic force microscopy (AFM), field emission scanning electron microscopy (FESEM), X-ray reflectivity (XR) and grazing-incidence small-angle X-ray scattering (GISAXS).

2. Experimental

2.1. Preparation of the thin films

Nanocrystalline pure zinc oxide films were obtained by sol–gel processing using a precursor solution composed of zinc acetate dihydrate dissolved in absolute ethanol, deionized water and acetic acid, as described in a previous work [7]. This solution was then deposited on amorphous SiO_2 flat substrates by applying several times the spin-coating technique during 10 s at 3000 rpm. In order

* Corresponding author. Tel.: +54 11 47098100x1212.
E-mail address: heredia.edu@gmail.com (E. Heredia).

http://dx.doi.org/10.1016/j.apsusc.2014.08.046
0169-4332/

to consolidate the deposited material after each deposition, the samples were subjected to partial heat-treatments during 10 min at 200 °C. This procedure led to the formation of thin films composed of 2, 4, 6 and 8 layers. Finally, the multilayered films were annealed during 3 h at 450 °C in order to achieve their whole crystallization and to eliminate organic residues.

2.2. Characterization techniques

The samples were studied by GIXD, by using a PW 3710 Philips diffractometer with Cu Kα radiation (wavelength λ = 1.542 Å), at a constant grazing incidence angle $\alpha_i = 1°$. The analysis of the GIXD patterns indicated that the thin films are crystalline, all the observed Bragg peaks corresponding to ZnO-wurtzite crystals. The average crystallite sizes, D, were determined from (1 0 0) and (1 0 1) peaks – the two most intense reflections – by applying Scherrer equation, $D = 0.9\lambda/(B\cos\theta_B)$, where B is the integral breadth (in radians) and θ_B the Bragg angle of the diffraction peak [8].

By applying the AFM technique, the root-mean-square surface roughness parameter, η_{AFM}, and the film thickness, t_{AFM}, were determined. The thickness was measured by determining the magnitude of the edge produced by scratching the thin films with a steel cutting tool. The AFM images were processed with the WSxM free software [9]. The thicknesses of the films were also determined from FESEM images of the cross-section perpendicular to the film surface.

XR and GISAXS experiments were performed using the D10A-XRD2 beam line of the LNLS synchrotron radiation facility, Campinas, Brazil, using a monochromatic 8 keV (λ = 1.549 Å) photon beam.

XR measurements were carried out using $\alpha - 2\alpha$ scans, by varying the α grazing incidence angle between 0.1° and 2°. In general, X-ray reflectivity patterns allow for determining the average density, the thickness and the roughness of the films by fitting a structure model to the experimental XR curve [10–12]. Since the XR patterns did not exhibit well-defined Kiessig fringes [13] the thickness could not be determined. Thus we have derived the average film densities from the values of the critical angle of total X-ray reflection.

The GISAXS technique was applied to determine the shape and the size distribution of pores in the nanometric scale embedded in the thin films. A KODAK imaging-plate was used to record the 2D GISAXS patterns. The grazing incidence angle of the X-ray beam was set at $\alpha_i = 0.4°$, slightly above the critical angle for total reflection of bulk ZnO ($\alpha_c = 0.33°$), for all the studied samples. The analysis of the GISAXS intensity was performed using the IsGisaxs 2.6 program [14].

3. Results

3.1. Grazing incidence X-ray diffraction

The GIXD patterns of the ZnO thin films deposited on silica glass Plates in the 2θ range between 30° and 39° – are plotted in Fig. 1. In order to compare the crystallographic parameters related to the crystalline structure of the different studied thin films, the GIXD patterns were determined by using identical experimental conditions. The angular positions of the Bragg peaks in the diffraction curves – (1 0 0), (0 0 2) and (1 0 1) reflections – are in agreement with those of the expected peaks for ZnO crystallites with wurtzite-like structure. These peaks are superposed to the diffuse scattering halo produced by the amorphous silica glass substrate.

The inset in Fig. 1 shows the added areas (Σ) of the three main peaks of ZnO. The added areas versus number of layers (n), $\Sigma \times n$ plots, indicate an approximately linear behavior. As the X-ray

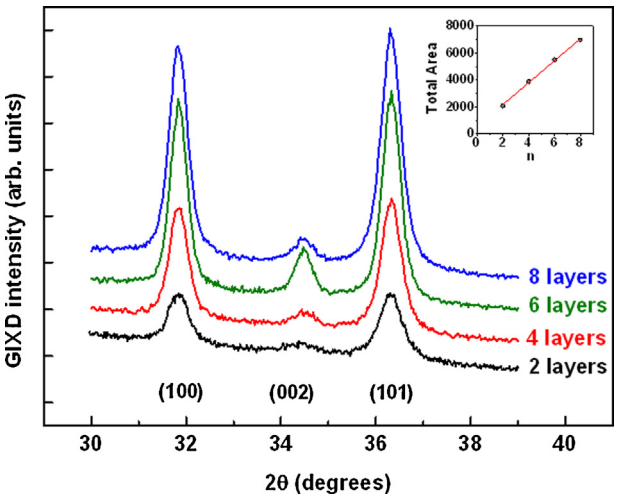

Fig. 1. GIXD diagrams of ZnO films carried out using Cu Kα radiation in grazing-incidence geometry (grazing incidence angle $\theta = 1°$). Inset: area of the diffraction peaks ($\Sigma = A_{(100)} + A_{(002)} + A_{(101)}$) versus the number of deposits, n.

absorption of the thin films here studied is weak, Σ is roughly proportional to the irradiated ZnO mass. Therefore, the behavior in the $\Sigma \times n$ curve in Fig. 1 indicates that nearly the same mass of ZnO is deposited in each layer.

The values of the average diameters of the ZnO crystallites D corresponding to the studied films, determined from the integral breadth of the main Bragg peaks after correction for instrumental broadening, are reported in Table 1.

3.2. Atomic force microscopy and field emission scanning electron microscopy

The morphology of the surface of the thin films can be seen in the AFM images shown in Fig. 2. In the upper left corner of all the images shown in Fig. 2 the distributions of the heights normal to the film surfaces are plotted. The root mean square parameters, η_{AFM}, were determined from these histograms using the WSxM software [9]. The results reported in Table 1 indicate that the magnitude of the roughness increases for increasing number of deposited layers, all values being within the 5–10 nm range. In the bottom right corner of each image in Fig. 2, we have plotted the profiles derived from AFM images corresponding to the thin film area after scratching it with a steel cutting tool. The thicknesses of the thin films determined by measuring the step depth of the grooves, t_{AFM}, are reported in Table 1, their values ranging from 43 to 147 nm.

Fig. 3 depicts the FESEM micrographs of the cross-section perpendicular to the ZnO thin film surfaces. In each image the regions corresponding to the film and substrate are clearly apparent. The thicknesses of the films, t_{FESEM}, obtained by 4, 6, and 8 successive spin-coating depositions are reported in Table 1. The thickness of the thinnest (2-layers) film could not be measured by FESEM because the image was blurry, this being probably due to a damaging of the thin film cross-section produced during the cutting process. The values of the thicknesses derived from FESEM measurements, t_{FESEM}, increase for increasing number of deposited layers, in good agreement with the observed trend of the thickness determined by AFM.

3.3. X-ray reflectivity

The XR patterns corresponding to samples with different numbers of ZnO deposited layers are plotted in Fig. 4. The reflectivity